Iranian Journal of Oil & Gas Science and Technology, Vol. 2 (2013), No. 2, pp. 65-76
http://ijogst.put.ac.ir

Failure Investigation of Hydrogen Blistering on Low-strength Carbon Steel

E. Shekari[1], M. R. Shishesaz[1*], Gh. Rashed[1], M. Farzam[1], and E. Khayer[2]

[1] Department of Technical Inspection Engineering, Petroleum University of Technology, Abadan, Iran
[2] Iranian Offshore Oil Company, Bahregan Oil District, Iran

Abstract

The current study assesses the root causes of hydrogen blisters on low strength carbon steel equipment. For this purpose, some experiments including hardness test, non-destructive test (NDT), metallography, and fractograpghy are conducted. The microstructure of two blisters is assessed by means of optical microscopy and scanning electron microscopy (SEM). The microstructural studies show that the steel plate has some inclusions and banded ferrite/pearlite structure. The energy dispersive x-ray spectroscopy (EDS) results indicate that these inclusions mainly contain Mn, S, Al, Ca, and Si. The results show that the inclusions and planar imperfections found in the NDT have been the nucleation locations for blisters in the plate. Remediation action plans are recommended to prevent further occurrence and growth of hydrogen blisters.

Keywords: Low-strength Carbon Steel, Hydrogen Blister, Storage Tank, Imperfection

1. Introduction

Low-strength carbon steels are widely used in refining industries for manufacturing pressurized components such as pipes and pressure vessels. Hydrogen blistering is a common form of hydrogen damage, which can occur throughout petrochemical industries in low-strength carbon steel pressurized components when a wet H_2S environment is present.

Hydrogen blisters may form as internal or external surface bulges or within the wall thickness of a pipe or pressure vessel. Blistering phenomenon occurs predominantly in low strength alloys when atomic hydrogen diffuses to internal defects such as laminations or nonmetallic inclusions and the hydrogen atoms combine to form hydrogen molecules that are too large to diffuse out; thus, the pressure builds up to the point at which local deformation occurs and thereby forming a blister. Hydrogen blisters can form at many different depths from the surface of the steel, in the middle of the plate, or near a weld. In some cases, neighboring or adjacent blisters that are at slightly different depths (planes) may develop cracks linking them together. Interconnecting cracks between the blisters, which is known as hydrogen induced cracking (HIC), often have a stair step appearance, and thus they sometimes are referred to as stepwise cracking. Vessels with a history of blistering are more susceptible to HIC than vessels with no history of blistering. Blisters are frequently found in low strength steels that have been exposed to aggressive corrosive environments (such as H_2S) or cleaned by pickling (Jatcak, 1956; Hirth, 1984; Mucek, 1999; Aleksanrov et al., 2003).

Aleksanrov and Chu have shown hydrogen-charged polycrystals of various materials suffered severe damage by blister and fissure formation (Aleksanrov et al., 2003; Chu et al., 2008). These results suggested that embrittlement was associated with the interaction of hydrogen and their impurities at

* Corresponding Author:
Email: shishesz@put.ac.ir

the grain boundary. Reasons for hydrogen-induced blistering and cracking have been investigated for several decades and have not clearly been solved yet (Chu et al., 2008; Ren et al., 2008). Many models of hydrogen-induced cracking in steel suggest that the hydrogen atoms diffuse to low free energy locations such as the interface of matrix and inclusions like manganese sulfides (MnS) (Krom et al., 1997; Ren et al., 2008). At these locations, the hydrogen atoms can combine to form hydrogen molecules that will exert a pressure on the surrounding steel, resulting in a crack. When the pressure in the crack exceeds a critical value (i.e. the pressure which results in a stress more than steel yield stress), the crack starts to grow.

Ren suggested a mechanism of hydrogen-induced micro-cracks in iron and steel according to which the hydrogen-induced propagations of internal cracks in iron and steel are promoted by hydrogen gas in voids or micro-cracks possibly formed by plastic deformation (Ren et al., 2008). It seemed likely that these micro-cracks originated from a dislocation pile-up as suggested by Stroh. In his model, the role of other kinds of hydrogen traps such as the second phase or inclusion particles was belittled. Chen suggested that the unhealed porosities in the ingot might be the source of flake formation (Chen et al., 1978). However, porosities are impossible in vacuum-floating zone-refining iron which can also flake if it is hydrogen charged.

Wilde observed the role of inclusion in the hydrogen-induced blister cracking of line pipe steels in sulfide environments and found that hydrogen-induced blister cracking initiated at elongated manganese sulfide and glassy silicate inclusions or massive columbium carbonitride precipitates (Wilde et al., 1980). Omizzi investigated the influence of sulfur content and inclusion distribution on hydrogen-induced blister cracking in pressure vessel and pipeline steels and found that HIC correlated with the elongated MnS inclusion (Omizzi et al., 2001). An extremely low sulfur level was not necessary to reach good HIC resistance, provided that no hard bands were present in the steel.

Ren investigated the relationship between the second phase and inclusion particles and the hydrogen-induced blisters of an industrial iron (Ren et al., 2007). They proposed an approach to the nucleation mechanism of hydrogen blisters as follows. Atomic hydrogen can induce superabundant vacancies in metals. The superabundant vacancies and hydrogen aggregate into a hydrogen-vacancy cluster (small cavity). The hydrogen atoms in the hydrogen-vacancy cluster change into hydrogen molecules that can stabilize the cluster and the hydrogen blister nucleates. The pressure in the small cavity increases as the hydrogen atoms enter the cavity. The cluster, which is the hydrogen blister nucleus, grows through vacancies diffusing into it under the action of cluster-hydrogen binding energy and hydrogen pressure. When the blister nucleus grows to a critical size, cracks will initiate from the wall of the cavity due to the internal hydrogen pressure.

Hydrogen blisters can be observed in numerous industries in which carbon steels are in contact with wet H_2S environment. For example, based on an interview with Research and Development Department of Abadan Oil Refining Company, this phenomenon has been observed in the catalytic reforming unit of this refinery. Also, according to the authors' experience in a research project in Esfahan Oil Refining Company, during last overhaul of the visbreaker unit of this refinery, scattered blisters were observed at the bottom of the heat exchangers. The occurrence of this phenomenon led to expending resources of time and money for grinding and eliminating surface blisters and overlay welding at these two refineries. Numerous hydrogen blisters have also been observed in a pipeline with ISO 3183 L360 (API 5L X52) material, transporting crude oil from the region of Bahregan oil district to Gore and Kharg Island.

The most striking example of this phenomenon, which is the subject of this investigation, is the occurrence of persistent hydrogen blisters in the oily water storage tanks in Bahregan oil district with a diameter of 21.30 m and having a capacity of 32,000 barrel. The tank has eight courses with thickness

varying from 12 mm at first bottom course to 6 mm at top four courses. The height of each course is 175 cm and the total height of the tank is about 14.00 m. Post weld heat treatment (PWHT) was conducted just on the reinforcing pad of the nozzles and man ways. The tanks are used for storing crude oil of Nowrooz, Soroush, Bahregan, and Hendijan fields. The oil stored in these tanks is sour and, based on daily measurements by on-site lab in Bahregan Oil District, the amount of input H_2S varies from 25 ppm to 100 ppm with the monthly average of 50 ppm. All blisters occurred on the second course of Tank #11 which had a nominal thickness of 10.66 mm. These blisters were found during a random in-service visual inspection of the tank. Some minor internal blisters and more than 10 hydrogen blisters in the outside surface were observed the diameter of one of which was 66 cm (see Figure 1).

The tank came into service in 1965. According to the tank inspection plan, it has been overhauled and fully inspected every 10 years. Based on the inspection procedure, the tank is drained in each turnaround and a full visual inspection of the internal surface is conducted after cleaning. The inspection procedure for the outside surface is full visual inspection and spot ultrasonic thickness measurement of specific points based on a thickness measurement sketch. Random visual inspection is also conducted between every subsequent tank overhaul at a maximum of every one year. The blisters were found during one of these random inspection in 2012, one year before the scheduled tank overhaul. No evidence of blisters was reported in the last tank overhaul conducted in 2003. Therefore, it can be concluded that the blisters had been generated in a nine year period between 2003 and 2012. As the random inspections between every subsequent tank overhaul did not cover the whole tank surface, it is not possible to estimate a tighter time period for the nucleation and growth of blisters. Due to the rigorous inspections implemented during the turnarounds, it can be said that no blisters had been generated in the first 35 years of the tank life.

This research attempts to fill the void related to a practical approach to decision making about equipment susceptible to hydrogen blisters. For this purpose, a case study on an oil storage tank in Bahregan oil district has been carried out by conducting required laboratory tests.

2. Experimental procedure

The purpose of this investigation was to determine the possible cause(s) of blister formation and also to identify any micro- or macro-defects inside the material. In this context, the following scope of laboratory tests was proposed:

- The visual examination and photographic documentation of the damaged plate in as-received conditions, followed by sectioning and sampling for further analysis by using hand saw cutting method to avoid any excessive generation of heat leading to a change in the microstructure;
- The cleaning and liquid penetrant testing (PT) of the blister to find possible crown cracks;
- The chemical composition analysis of parent metal using the optical emission spectroscopy (OES) technique;
- Hardness survey at the locations of intact sample;
- The ultrasonic examination (UT) of the intact sample for the exact determination of the location of possible internal defects followed by magnetic particle examination of the sample plate edges to validate the results of the ultrasonic examination for those types of identified defects near the plate edges;
- Sample grounding and polishing according to ASTM E3-11 (2011) and etching the sample at room temperature in a 2% Nital solution;
- The micro structural examination of the damaged plate at blister locations.

- The fracture surface investigation of the fracture surface of a sample blister using scanning electron microscopy (SEM).

3. Results and discussion

3.1. Visual examination

Figure 1 shows the storage tank shell course from which the section was extracted. A reddish brown corrosion deposit/extract was observed on the internal surface of the plate. A sample with a cross sectional area of 300 mm (width) by 600 mm (length) and a nominal wall thickness of 10.66 mm was extracted from the intact area of the second course plate near the damaged area for conducting non-destructive evaluation (NDE), chemical composition, and hardness tests; the locations are shown in Figure 1. Furthermore, two blisters (the smallest blister found during the internal inspection and another larger external blister near it) were selected for microstructural examination and fracture surface investigation as shown in Figure 1. The reason for selecting one small and one large blister was to conduct further studies on the fracture behavior of the plate during the blister growth.

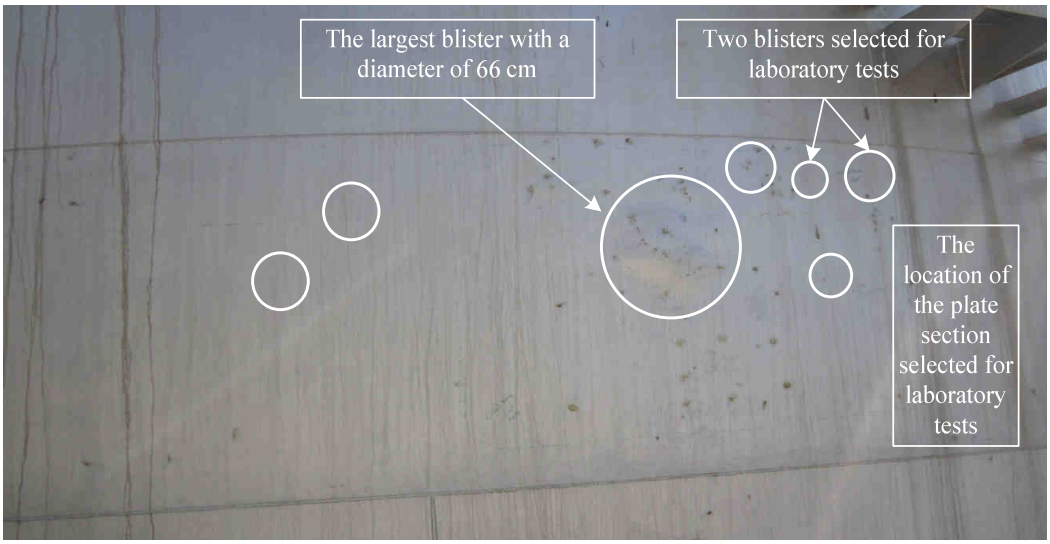

Figure 1
The damaged second course plate before repair

3.2. NDT examination

UT was conducted on the selected section near the blistered area using normal straight UT equipment. The plate was thoroughly inspected by visual examination before UT to ensure that no blisters were present. The plate was marked into smaller areas as shown in Figure 2. The UT report revealed planar imperfections distributed throughout the plate. These imperfections were distributed in zones B, D, E, G, and H with different depths from 7 to 9 mm measured from the outside surface (outside diameter) of the tank (see Figure 2).

Magnetic particle inspection (MPI) based on Yoke method was also conducted on all the four edges of the sample to validate the results of the UT and also to investigate the probable extension of the planar defects toward the edges of the sample (i.e. toward other areas of the shell course). Cutting and edge preparation was conducted by grinding to avoid overheating and metallurgical changes of the plate edges; fluorescent magnetic powder was used. All the edge surfaces were investigated in different directions of magnetic flux under UV light. Several planar, crack-like flaws were observed at different depths varying from 7 to 9 mm from the outside surface of the tank. The results of the MPI tests were

compared with the UT results.

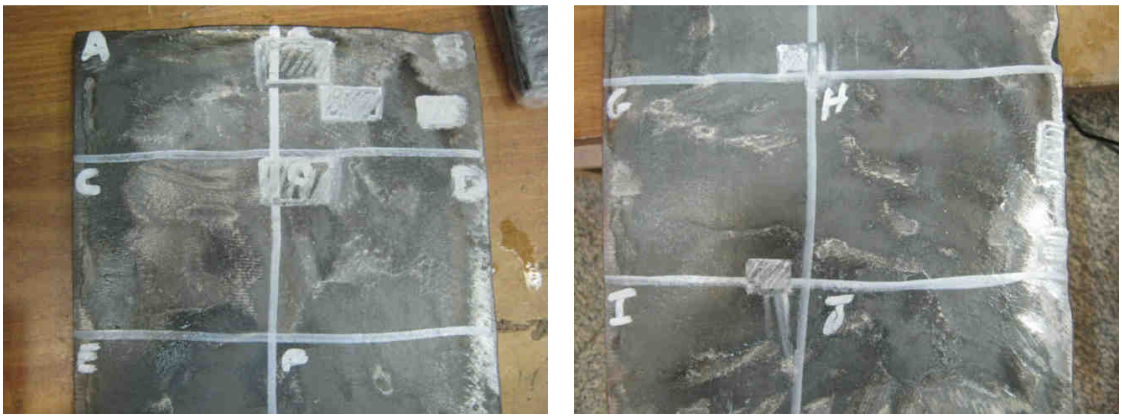

Figure 2
A sample plate was divided into different zones to conduct UT

3.3. Chemical composition analysis

The chemical composition analysis of a representative sample from base metal was performed using OES technique. The results of the analysis are shown in Table 1. The chemical composition of the sample plate was consistent with the requirements of the ASA 52. This standard is currently outdated and steel plate UNS No. K02700 (ASTM A516 Grade 70) is being used in Bahregan oil district for any required repairs. Table 2 shows the chemical requirements of ASTM A516 Grade 70. As can be seen by comparing Tables 1 and 2, except for Mn with small deviation, the results of chemical composition analysis are consistent with ASTM A516 Grade 70.

Table 1
Chemical composition analysis of a representative sample

C %	Si %	Mn %	P %	S %	Cr %	Ni %	Mo %	Cu %	V %	W %
0.20±0.02	0.04	0.63	0.027	0.025	0.09	0.08	0.02	0.16	Trace	Trace
Ti %	**Co %**	**Al %**	**Sn %**	**Pb %**	**As %**	**Sb %**	**Zr %**	**Nb %**	**Mg %**	**Fe %**
Trace	0.01	None	0.02	None	0.03	0.01	Trace	Trace	-	Base

Table 2
Chemical requirements of ASTM A516 (Grade 70)

Carbon, max	Manganese	Phosphorus, max	Sulfur, max	Silicon
0.27	0.79–1.30	0.035	0.035	0.13–0.45

3.4. Hardness test

The Brinell hardness test was done according to ASTM E 10-10 on a sample of the storage tank intact plate. The average of three hardness tests done on the sample was 145 HB. According to API 571 and API 579 classification, this hardness is consistent with low-strength steel category, i.e. hardness less than Brinell 237 (API, 2007). However, based on API 571 2011, steel hardness is not a critical factor for blister nucleation and growth; this test was conducted here mainly with the purpose of material verification.

3.5. Metallographic examination

A representative sample was extracted from the periphery of the smaller blister (i.e. the tip of the

blister crack) to conduct metallographic examination.

Figure 3
A metallographic examination sample extracted from the periphery of the blister (crack tip)

Figure 4 shows the results of the metallographic examination of the sample. At first, an optical microscope study was performed on the polished sample (Figures 4.a). Then, an image was taken of the etched sample with an optical microscope (Figures 4.b). The images were taken of the tip of crack and its boundary.

In Figures 4.a some scattered inclusions can be observed elongated in rolling direction. As will be discussed later in energy dispersive spectroscopy (EDS) results, these inclusions mainly include S and Mn as well as other inclusions. These inclusions can also be seen at the tip of the cracks and their boundaries. As reported by Ren, inclusions are an important factor in the propagation of initiated cracks and the growth of the hydrogen blisters (Ren et al., 2008).

Ferrite grains (of a size of 7 to 10 G according to ASTME 112-10) and needle-like ferrites beside pearlite grains and elongated pearlite were detected in Figure 4.b (ASTM, 2000). As it can be seen, there are ferrite/pearlite banding. The progression of cracks is parallel to the banding perlite and follows that; however, its amount is low in this structure. Moreover, the transgranular cracks are seen and this indicates that embrittlement phenomenon may be occurred in some locations. Not only do cracks propagate in inclusion path, they grow among grains as well.

Banded pearlites are susceptible locations for the progression of cracks. Cracks tend to follow pearlite bands as well as elongated sulfides; even cracks in different bands may link up. This means that a higher elongated inclusion, or a more banding, increases steel susceptibility to HIC in a wet acidic environment (Dadari, 2011).

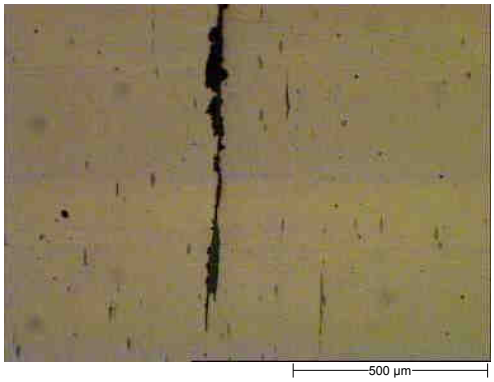

a. Propagation of a crack and scattered distribution of inclusions

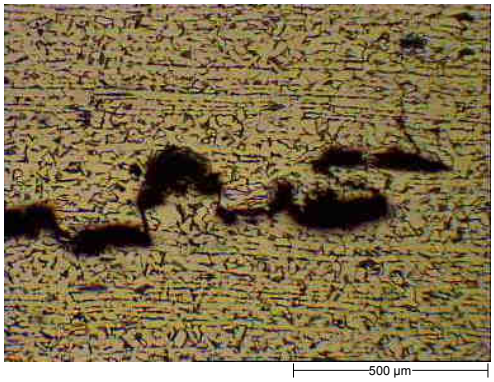

b. Tip of a crack and a transgranular crack

Figure 4
Metallographic examination results

3.6. Fractographic investigation

To investigate the fracture surface of blisters, following samples were extracted:

- Samples No. 2 and No. 3 from the fracture surface of a smaller blister;
- Samples No. 4 and No. 5 from the fracture surface of a larger blister.

These samples were selected from two opposite sides of the fracture surface of each blister (i.e. two samples in front of each other from the fractured surface of each blister). The SEM images of the samples of the small blister are shown in Figures 5 and 6; Figures 8 and 9 show the SEM images of the samples of the large blister. The EDS results are also shown in Figure 7 and 10 for the small and large blisters respectively.

A brittle fracture can be seen in Figures 8 and 9 (the small blister) and Figures 11 and 12 (the large blister). At the same time, a case of a mixed small ductile and brittle fracture can be seen in Figure 9.b and c which are related to the smaller blister. For the case of Figure 6 with a mixed ductile-brittle surface, it can be concluded that hydrogen was present in a lower content (Herms et al., 1999).

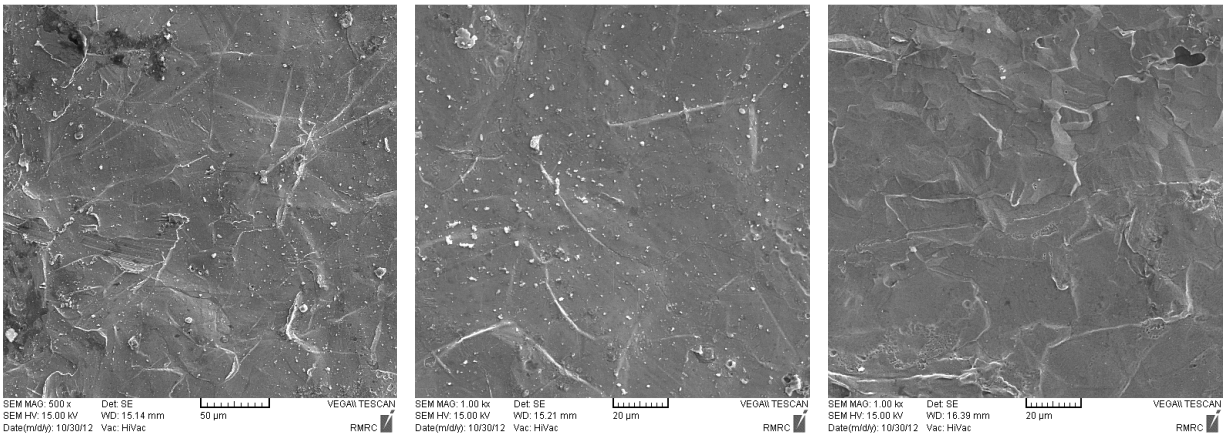

(a) brittle fracture (magnification 500x) (b) brittle fracture (magnification 1000x) (c) brittle fracture (magnification 1000x)

Figure 5

SEM images of fracture surfaces related to sample No. 4 (the small blister)

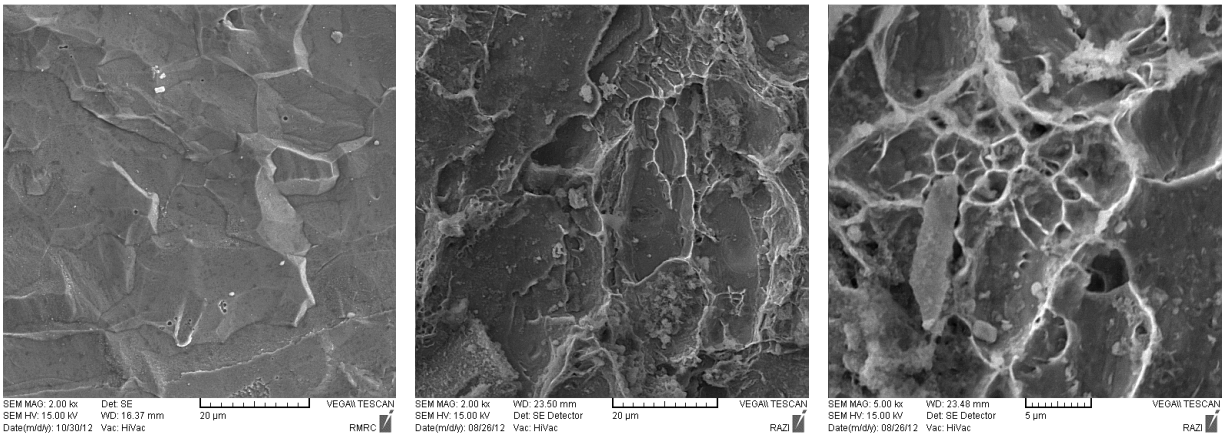

(a) brittle fracture (magnification 2000x) (b) Mixed ductile and brittle fracture (magnification 2000x) (c) Mixed ductile and brittle fracture (magnification 5000x)

Figure 6

SEM images of fracture surfaces related to sample No. 5 (the small blister)

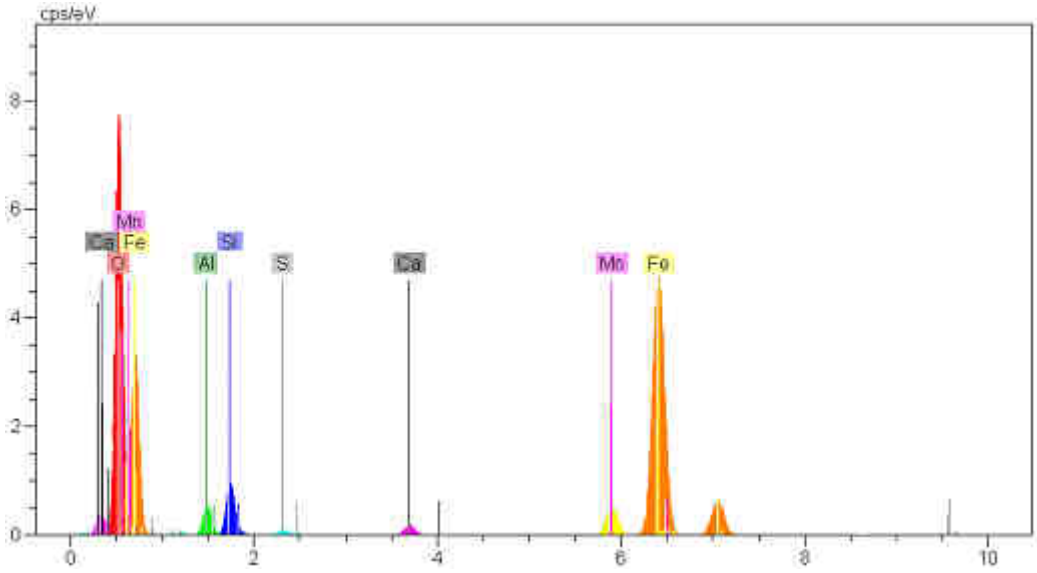

Element	unn. C [wt.%]	norm. C [wt.%]	Atom. C [at.%]
Iron	74.09	70.36	46.23
Manganese	6.23	5.92	3.95
Calcium	0.60	0.57	0.52
Sulfur	0.27	0.26	0.30
Silicon	2.34	2.22	2.90
Aluminum	1.49	1.41	1.92
Oxygen	20.28	19.26	44.17

Figure 7
EDS result from the fracture surface of the small blister

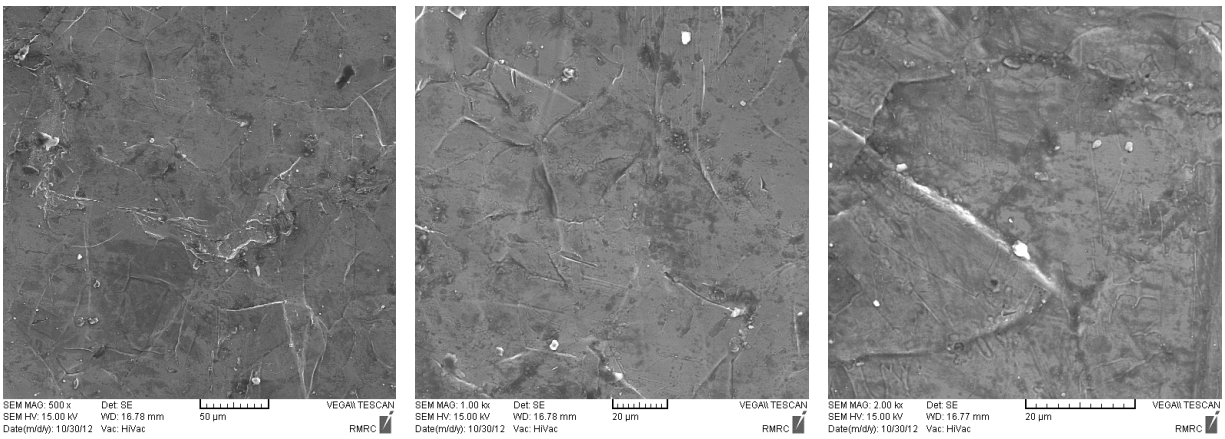

(a) brittle fracture (magnification 500x) (b) brittle fracture (magnification 1000x) (c) brittle fracture (magnification 2000x)

Figure 8
Fracture surface of sample No. 6 (the large blister)

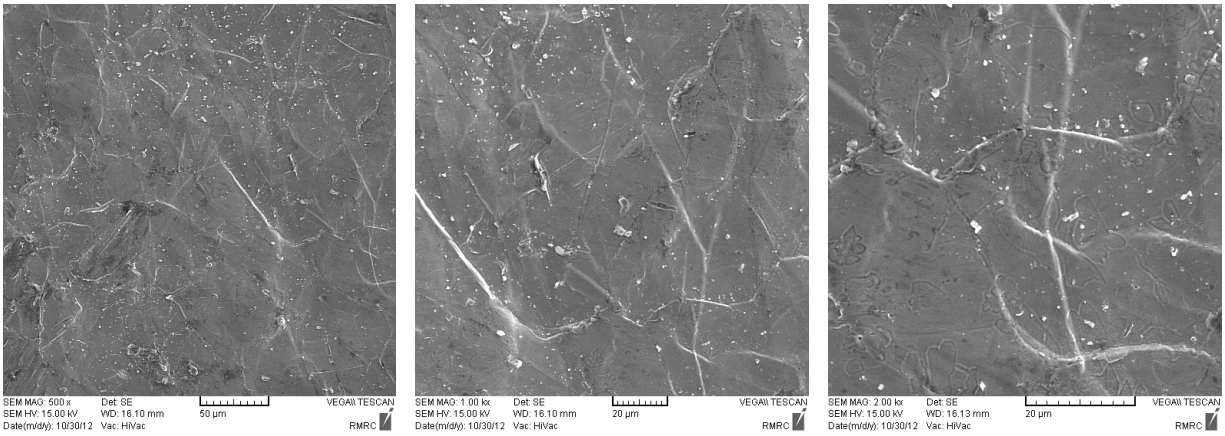

(a) (magnification 500x) (b) (magnification 1000x) (c) (magnification 2000x)

Figure 9
Fracture surface of sample No. 7 (the large blister at another location)

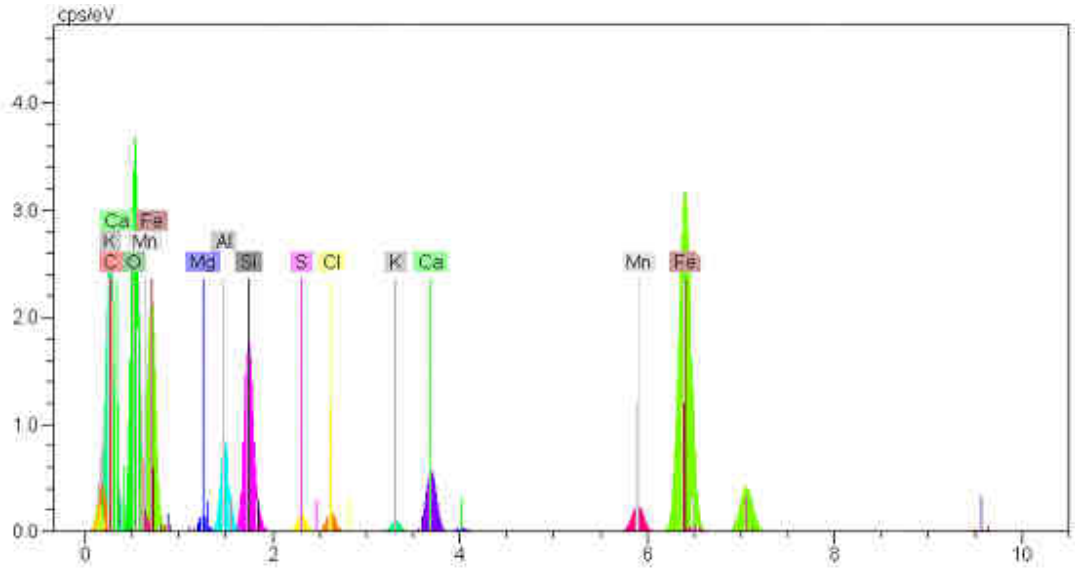

Element	unn. C [wt.%]	norm. C [wt.%]	Atom. C [at.%]
Iron	60.04	60.67	39.07
Manganese	3.24	3.58	2.34
Calcium	2.10	2.33	2.09
Sulfur	0.42	0.47	0.52
Silicon	4.68	5.17	6.63
Chlorine	0.43	0.47	0.48
Aluminum	2.28	2.52	3.36
Oxygen	15.89	17.58	39.51
Carbon	0.52	0.58	1.72
Potassium	0.31	0.34	0.31

Figure 10
EDS result of the fracture surface related to the larger blister

It can be inferred from Figures 6.a, 8, and 9 that a step like pattern and cleavage can be seen in the fracture surface of the samples which can represent a brittle fracture. However, there are some locations not following this structure. These locations are inclusions. To satisfy this assumption, EDS was done on the samples. The EDS results (shown in Figures 7 and 10) indicate that these inclusions mainly contain Mn, S, Al, Si, and Ca.

Theories for hydrogen damage include the pressure theory, the surface adsorption theory, decohesion, enhanced plastic flow, hydride formation, and hydrogen attack. Pressure theory, apparently reasonable for blistering and possibly appropriate for some aspects of loss in tensile ductility, does not explain many of the factors observed for classes of failures. However, it is a well-recognized phenomenon that charging hydrogen into steel or nickel alloys at high fugacity, either with high-pressure hydrogen gas or under extreme electro-chemical charging, can create a significant density of voids and irreversible damage to the alloy consistent with a pressure-dependent model (ASM Handbook Committee, 2003).

As it was mentioned, blistering occurs predominantly in low-strength alloys and it results from hydrogen atoms that form during the sulfide corrosion process on the surface of the steel, diffuse into the steel, and collect at a discontinuity in the steel such as an inclusion or lamination. Similar findings are also reported by API 579-1 (API, 2007). The hydrogen accumulates and results in the build-up of high pressure that causes local stresses that exceed the yield strength of the material near these imperfections. The pressure of molecular hydrogen can attain such high values that localized plastic deformation of the alloy occurs, forming a blister that often ruptures. Blisters are frequently found in low-strength steels that have been exposed to aggressive corrosive environments (such as H_2S) or cleaned by pickling.

In iron and steel, S usually exists as MnS (Ren et al., 2008). So, most probably Mn and S are in the form of MnS being outspread in the background of the structure. From Figure 4, MnS and most of other inclusions have an elongated shape. The probability of inclusions containing Al, Si, and Ca is also high in the structure according to the EDS results. Si in the form of SiO_2 can tightly bond with hydrogen (Ren et al., 2008). Al may be in the form of alumina, alumina silicate and also Al_2O_3 (Ren et al., 2008). These inclusions are susceptible locations for trapping the diffused hydrogen and the initiation of the cracks and therefore they are the nucleation sites of hydrogen blisters. These inclusions can enter to base alloy in casting and rolling of plates.

Because of the corrosion reaction occurring on the inner surface, the sour oil inside the storage tank is capable of evolving atomic hydrogen. Since the internal surface of the tank does not have a coating, the hydrogen penetrates into the metal. As mentioned in API 571 and API 579-1/ASME FFS-1 (ASME, 2007), the elimination or reduction of hydrogen charging by means of a barrier coating (e.g. organic coatings), or by changing the process environment could be effective in avoiding further blister generation and/or growth of existing blisters. Several inclusions and planar defects inside the base metal found during NDE, metallographic experiments, and EDS are susceptible locations to trap the molecular hydrogen. As there was no evidence of blisters of any size in previous overhaul inspections and in-service random visual inspections and due to the large size of the existing blisters, it can be concluded that the blisters would grow rapidly once formed.

Since the other plates in this tank have the same material and same fabrication conditions, it is recommended to apply an internal coating to eliminate or reduce the hydrogen charging in order to prevent further generation and growth of blisters. In addition, reducing the S content to 0.002 or 0.005%, using heat treatment processes to eliminate the banding (in new plates and in the whole tank plates on site), and employing steel grades with 0.2% Cu are suggested for preventing this kind of failure in the future.

4. Conclusions

- Based on the experiments results, inclusions (most likely sulfide inclusions such as MnS, Al, and Si) and planar imperfections (such as laminations resulting from plate fabrication and rolling) in the plate have been the nucleation locations for blisters;
- Ferrite and pearlite banding indicated in structure seems to facilitate the propagation of blisters;
- According to the NDE results, the size of the planar defects were considerable which, in conjunction with H_2S content in the tank, caused the rapid growth of blisters and generated large diameter damaged areas.

The results of this research illustrate the importance of plate manufacturing and pre-fabrication tests for detecting internal imperfections. In this case study, the blister damage would not probably be occurred if appropriate NDE with proper coverage had been carried out on the plates before the fabrication of the tank to detect the pre-existing imperfections.

Acknowledgements

The authors would like to express their appreciation to the R&D Department of Iranian Offshore Oil Company for their technical support and the R&D Department of Abadan Oil Refining Company for their financial support during this research. A word of thanks also goes to Dr. Ashrafi from Shahid Chamran University for his valuable suggestions and helpful discussion throughout this work.

Nomenclature

ASTM	: American society for testing and materials
EDS	: Energy dispersive x-ray spectroscopy
HIC	: Hydrogen induced cracking
MPI	: Magnetic particle inspection
NDE	: Non-destructive evaluation
NDT	: Non-destructive test
PT	: Penetrant testing
PWHT	: Post weld heat treatment
SEM	: Scanning electron microscopy
UT	: Ultrasonic examination
wt.%	: Weight percent

References

Aleksandrov, R. E. P. A., Baranova, E. K., Baranova, I. V., Defects Solids, p. 771, 2003.

American Petroleum Institute, API 579-1/ASME FFS-1, Fitness for Service, 2nd Ed., Washingtion, USA, 2007.

ASTM 112, Standard Test Methods for Determining Average Grain Size, 1, 2000.

ASM Handbook Committee, ASM Metals Handbook Volume 11, Failure Analysis and Prevention. 2002.

ASM Handbook Committee, ASM Metals Handbook Volume 13A, Corrosion: Fundamentals, Testing, and Protection. Houston, TX, ASM International, 2003.

ASTM E3-11 Standard Guide for Preparation of Metallographic Specimens, 2011.

API571, Damage Mechanisms Affecting Fixed Equipment in the Refining Industry, 2nd Ed., Washingtion, USA, API, 2011.

Chen, W. Q. Y. L., Xu, Y. B., Acta Metallurgican Sinka, Vol. 14, p. 253, 1978.

Dadari G., Failure Analysis of Sludge Catcher in Tange Bijar Field (Ilam), Petroleum University of Technology, MSc. Thesis, 2011.

Herms, E., Olive, J., and Puiggali M., Hydrogen Embrittlement of 316L-type Stainless Steel, Materials Science and Engineering, Vol. 272, No. 2, p. 279-283, 1999.

Hirth, J. P., Theories of Hydrogen Induced Cracking, Hydrogen Embrittlement and Stress Corrosion Cracking, Ohio, USA, p. 29-41, 1984.

Jatcak, C. F., Girardi, D. J., and Rowland, E. S., Trans. ASM, Vol. 48, p. 279-305, 1956.

Krom, A. H. M. and Bakker, A., Modeling Hydrogen-induced Cracking in Steel Using a Coupled Diffusion Stress, International Journal of Pressure Vessels and Piping, Vol. 72, p. 139-147, 1997.

Mucek, M. W., Detection, Repair, and Mitigation of Wet H_2S Cracking: an Overview of RP0296, NACE Corrosion/99, 1999.

Omizzi, J. O. G. G. D., Anteri, G., Corros. Sci., Vol. 43, p. 325, 2001.

Ren, X., Chu, W., Li, J., Su, Y., and Qiao, L., The Effects of Inclusions and Second Phase Particles on Hydrogen-induced Blistering in Iron Materials Chemistry and Physics, Vol. 107, No. 2-3, p. 231-235, 2008.

Ren, X. C., Zhou, Q. J., Shan, G. B., Chu, W. Y., Li, J. X., Su, Y. J., and Qiao, L. J., A Nucleation Mechanism of Hydrogen Blister in Metals and Alloys, Metallurgical and Materials Transactions, Vol. 39, No. 1, p. 87-97, 2007.

Wilde, E. H. P. B. E. and Kim, C. D., Corrosion, Vol. 36, p. 625, 1980.